Net electron acceleration by a strong laser field and a rf wave

Liang Feng
T. D. Lee Physics Laboratory, Fudan University, Shanghai 200433, China

Yu-Kun Ho*
China Center of Advanced Science and Technology (World Laboratory), P.O. Box 8730, Beijing 100080, China and T. D. Lee Physics Laboratory, Fudan University, Shanghai 200433, China

(Received 15 July 1993)

Net electron acceleration by the coupling of a comoving laser and a counterpropagating rf wave in the presence of an additional longitudinal electrostatic field is investigated. The trajectories of electrons in the phase space of the ponderomotive potential of the combined fields are given analytically. A striking feature of the interaction compared to that in the absence of the electrostatic field [Phys. Rev. E **47**, R2277 (1993)] is that the symmetry of electron trajectories in the phase space is broken, which could result in a net acceleration. Numerical results indicate that with an electrostatic field of intensity 1×10^5 V/cm incorporated, electrons can get a net acceleration from 45 to 95 MeV over 4.8 cm in the combined fields formed by a laser beam with electric intensity 1×10^{10} V/cm and wavelength 1.06 μm, and a rf field with electric intensity 10^5 V/cm and wavelength 10.6 cm. The averaged net acceleration gradient is about 1×10^3 MeV/m.

PACS number(s): 41.75.Fr, 29.17.+w, 41.85.−p, 42.62.Hk

I. INTRODUCTION

Recent technological advances have made it possible to produce an electric field as high as 10^{11} V/cm with powerful focused lasers, which stimulates significant interest in the use of lasers to accelerate electrons. By now, there have been many papers devoted to the investigation of various schemes for laser-based accelerators [1–11]. Among these schemes, the inverse free-electron-laser accelerators (IFEL's) and the plasma-wave accelerators are more extensively studied.

In our recent paper [1], a backward (relative to the electron motion) traveling electromagnetic wave (rf wave) is used to replace the magnetostatic wiggler in the conventional IFEL's. The feature of this scheme is that the phase speed of the ponderomotive potential formed by the beating of the laser and rf wave is slower than c, the velocity of light in vacuum, resulting in a favorable situation in which the phase matching of the electrons with the potential can be maintained over a longer distance and the electrons can lose or acquire more energy from the radiation fields. However, the critical problem of this kind of laser-based accelerator is how to get net acceleration. As mentioned in the literature [1,11], due to the symmetry of electromagnetic waves in free space and the fact that the velocities of electrons are slower than c, the electrons would undergo alternately acceleration and deceleration. Therefore, no net energy exchange would take place, if the interaction length is unlimited. In order to achieve net acceleration, some proposals have been made. One of them is to limit the interaction length by assuming that it were possible to inject and remove electrons from the acceleration field in exactly correct positions (for example, use a moving thin foil to terminate the interaction or use a strong transverse static magnetic field to bend abruptly the electron trajectory from the radiation field [12]).

In this article, we explore an alternative proposal where an additional electrostatic field is applied along the longitudinal direction to break the symmetry of the ponderomotive potential in the phase space and, consequently, achieve net acceleration. A comparison of the IFEL experiments with and without an incorporation of the external electrostatic field could be of interest to test the electron dynamics underlying the IFEL setups. Also, the proposed interaction may be viewed as a two-beam-assisted inverse bremsstrahlung, which is of current research interest [13,14]. In Sec. II we will find the analytical solution of electron motion in the phase space of the ponderomotive potential. Section III is devoted to proving the possibility of achieving net electron acceleration in the presence of electrostatic field. Section IV is a brief summary.

II. ELECTRON DYNAMICS

We begin by studying the motion of electrons in the configuration shown in Fig. 1. As in Ref. [1], we take the laser beam and the backward rf wave both to be uniform and circularly polarized plane waves with vector potentials

*Address for correspondence: Physics Department 2, Fudan University, Shanghai 200433, China.

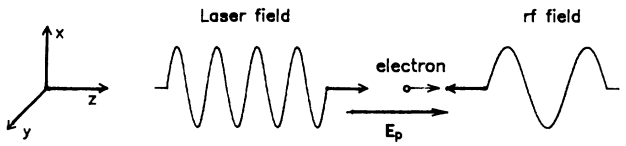

FIG. 1. Configuration for net electron acceleration in the laser and rf wave in the presence of an additional longitudinal electrostatic field E_p.

$$\mathbf{A}_0 = A_0(\hat{\mathbf{x}}\cos\phi + \hat{\mathbf{y}}\sin\phi) , \tag{1}$$

$$\mathbf{A}_1 = A_1(\hat{\mathbf{x}}\cos\eta + \hat{\mathbf{y}}\sin\eta) , \tag{2}$$

where $\phi = \omega_0 t - k_0 z$, $\eta = \omega_1 t + k_1 z + \phi_0$; $[\omega_0, \mathbf{k}_0(0,0,k_0)]$ and $[\omega_1, \mathbf{k}_1(0,0,-k_1)]$ denote the frequencies and wave vectors of the laser and rf field, respectively; ϕ_0 designates the initial phase of the laser field; A_0 and A_1 represent the amplitudes of the two potentials; and $\hat{\mathbf{x}}$, $\hat{\mathbf{y}}$, and $\hat{\mathbf{z}}$ are the unit vectors along the x,y,z axes, respectively. In the presence of a homogeneous longitudinal electrostatic field $E_p\hat{\mathbf{z}}$, the motion of a relativistic electron with mass m_0 and charge q is determined by

$$\frac{d\mathbf{P}_\perp}{dt} = -q\frac{d(\mathbf{A}_0 + \mathbf{A}_1)}{dt} , \tag{3}$$

$$\frac{d\mathbf{P}_z}{dt} = -q\mathbf{V}_\perp \times (\mathcal{B}_0 + \mathcal{B}_1) + qE_p\hat{\mathbf{z}} , \tag{4}$$

$$m_0c^2\frac{d\gamma}{dt} = q(\mathcal{E}_0 + \mathcal{E}_1)\cdot\mathbf{V}_\perp + qE_pV_z , \tag{5}$$

where $\mathcal{E}_0(\mathcal{E}_1)$ and $\mathcal{B}_0(\mathcal{B}_1)$ are the electric and magnetic fields of the laser (rf wave), the subscript $\perp$ denotes the transverse component of the electron momentum $\mathbf{P}$ and the velocity $\mathbf{V}$, and γ is the Lorentz factor.

By integrating Eq. (3) and inserting it in Eqs. (4) and (5), one obtains

$$\mathbf{V}_\perp = -\frac{q}{m_0\gamma}(\mathbf{A}_0 + \mathbf{A}_1) , \tag{6}$$

$$\frac{d\gamma}{dt} = \left[\frac{qA_0}{m_0c}\right]\left[\frac{qA_1}{m_0c}\right]\frac{1}{\gamma}(\omega_0 - \omega_1)\sin\psi + \frac{qE_p}{m_0c}\beta_z , \tag{7}$$

$$\frac{d\beta_z}{dt} = \left[\frac{qA_0}{m_0c}\right]\left[\frac{qA_1}{m_0c}\right]\frac{1}{\gamma^2}[\omega_0(1-\beta_z) + \omega_1(1+\beta_z)]\sin\psi + \frac{qE_p}{\gamma m_0c}(1-\beta_z^2) , \tag{8}$$

where $\beta_z = V_z/c$, $\psi = (\omega_1 - \omega_0)t + (k_1 + k_0)z + \phi_0$ is the particle phase in the field. The phase velocity of the ponderomotive potential formed by the beating of two waves is given by

$$V_\psi = \frac{\omega_0 - \omega_1}{\omega_0 + \omega_1}c . \tag{9}$$

For $\omega_1/\omega_0 = 1\times10^{-5}$, it yields $\beta_\psi = V_\psi/c = 0.999\,98$.

From Eqs. (7) and (8), one may obtain

$$\frac{d\left\{\gamma\left[\left[1+\frac{\omega_1}{\omega_0}\right] - \left[1-\frac{\omega_1}{\omega_0}\right]\beta_z\right]\right\}}{dt} = \frac{qE_p}{m_0c\omega_0}\frac{d\psi}{dt} . \tag{10}$$

Here we define a function of ψ,

$$\mathcal{K}(\psi) = \gamma\left[\left[1+\frac{\omega_1}{\omega_0}\right] - \left[1-\frac{\omega_1}{\omega_0}\right]\beta_z\right] , \tag{11}$$

and the integration of Eq. (10) yields

$$\mathcal{K}(\psi) = \mathcal{K}(\psi_0) + \frac{qE_p}{m_0c\omega_0}(\psi - \psi_0) , \tag{12}$$

where ψ_0 designates the initial value of ψ. By using Eq. (6), one may rewrite Eq. (11) as

$$\left[(1-\beta_z) + \frac{\omega_1}{\omega_0}(1+\beta_z)\right]\frac{1}{(1-\beta_z^2)^{1/2}} = \frac{\mathcal{K}(\psi)}{\left[1+\left[\frac{q}{m_0c}\right]^2(A_0^2 + A_1^2 + 2A_0A_1\cos\psi)\right]^{1/2}} . \tag{13}$$

By setting

$$\frac{\mathcal{K}(\psi)}{\left[1+\left[\frac{q}{m_0c}\right]^2(A_0^2 + A_1^2 + 2A_0A_1\cos\psi)\right]^{1/2}} = \alpha(\psi) , \tag{14}$$

one solves for β_z from Eq. (13),

$$\beta_z = \frac{1 - \left[\frac{\omega_1}{\omega_0}\right]^2 \pm \alpha(\psi)\left[[\alpha(\psi)]^2 - 4\left[\frac{\omega_1}{\omega_0}\right]\right]^{1/2}}{[\alpha(\psi)]^2 + \left[1-\left[\frac{\omega_1}{\omega_0}\right]\right]^2} . \tag{15}$$

Inserting Eq. (15) into Eq. (10), one also has

$$\gamma = \mathcal{K}(\psi)\frac{\left[1+\frac{\omega_1}{\omega_0}\right]\alpha(\psi) \pm \left[[\alpha(\psi)]^2 - 4\left[\frac{\omega_1}{\omega_0}\right]\right]^{1/2}\left[1-\frac{\omega_1}{\omega_0}\right]}{4\left[\frac{\omega_1}{\omega_0}\right]\alpha(\psi)} . \tag{16}$$

Comparing Eq. (15) with Eq. (18) of Ref. [1], we find that these two formulas are of a similar form. The difference between them is that in the presence of electrostatic field the constant $\mathcal{K}_2$ in Eq. (18) of Ref. [1] is replaced by a function $\mathcal{K}(\psi)$, which is linearly related to the phase ψ by Eq. (12).

III. NET ACCELERATION

Next we examine the influence of the applied electrostatic field on the electron trajectory in the phase space. Figure 2 depicts the phase plots of electron trajectories in the P_z-ψ plane with wave field parameters $\omega_1/\omega_0=10^{-5}$, $E_0=1\times10^{10}$ V/cm, and $E_1=1\times10^5$ V/cm. The dot-dashed line represents the diagram in the absence of electrostatic field, where the whole P_z-ψ plane is divided into three regions. The solid lines which represent the diagram in the presence of electrostatic field, delimit the P_z-ψ plane into four regions $\mathcal{D}_1$ to $\mathcal{D}_4$. The electron trajectories in the regions $\mathcal{D}_1$–$\mathcal{D}_3$ are similar to that without the electrostatic field, but shift rightward in the phase plane. The region $\mathcal{D}_4$ represents a new electron dynamic scenario caused by the incorporation of electrostatic field. Formally, the electron trajectories in different regions may be discriminated by the number of resonant points, where $\beta_z=\beta_\psi$, in the interval $\psi=0-2\pi$. (Exactly, this region is shifted by the electrostatic field to $-\psi_r\le\psi\le2\pi-\psi_r$, where ψ_r is determined by

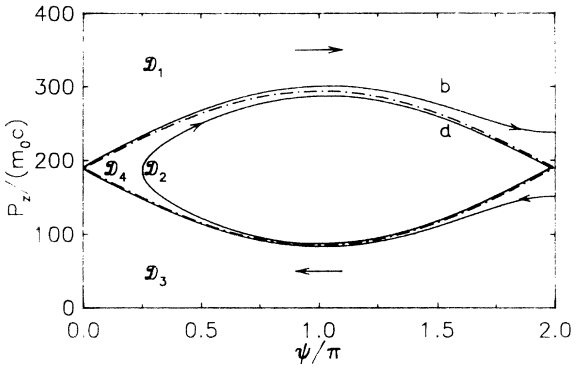

FIG. 2. Phase plots for electron trajectories in the configuration shown in Fig. 1. The adopted field parameters are $\lambda_0=1.06$ μm, $\lambda_1=10.6$ cm, $E_0=1\times10^{10}$ V/cm, and $E_1=10^5$ V/cm. The dot-dashed line represents the phase boundary in the absence of electrostatic field (see Ref. [1]). The solid lines b and d divide the whole phase space into four regions $\mathcal{D}_1$, $\mathcal{D}_2$, $\mathcal{D}_3$, and $\mathcal{D}_4$. $\mathcal{D}_4$ is the region of most concern in this article, where electrons might achieve net acceleration.

$$\psi_r=\arcsin\left\{\left[\frac{E_p}{2\omega_0A_0}\right]\left[\frac{m_0c}{qA_1}\right]\left[\frac{1+\beta_\psi}{1-\beta_\psi}\right]^{1/2}\left|1+\left[\frac{q}{m_0c}\right]^2(A_0^2+A_1^2+2A_0A_1\cos\psi_r)\right|^{1/2}\right\}. \tag{17}$$

Normally, the value of ψ_r is tiny, and will be ignored in the following. For example, when $qE_p=10^5$ eV/cm, ψ_r is about 0.006 rad.) The number of resonant points is zero, two, zero and one for a trajectory in the region $\mathcal{D}_1$, $\mathcal{D}_2$, $\mathcal{D}_3$, and $\mathcal{D}_4$, respectively.

From Eq. (15), the resonant condition is given by

$$[\alpha(\psi_s)]^2-4\left[\frac{\omega_1}{\omega_0}\right]=0\ , \tag{18}$$

where ψ_s denotes the value of the particle phase ψ satisfying the equation $\beta_z=\beta_\psi$. Recalling Eq. (14), note that the value of ψ_s is determined by

$$\psi_{s1}=\arccos\left\{\frac{m_0^2c^2}{2q^2A_0A_1}\left[\frac{\omega_0}{4\omega_1}[\mathcal{K}(\psi_{s1})]^2-\left[1+\frac{q^2}{m_0^2c^2}(A_0^2+A_1^2)\right]\right]\right\}, \tag{19}$$

for $\sin(\psi_{s1})>0$ $(0\le\psi_{s1}<\pi)$, or

$$\psi_{s2}=2\pi-\arccos\left\{\frac{m_0^2c^2}{2q^2A_0A_1}\left[\frac{\omega_0}{4\omega_1}[\mathcal{K}(\psi_{s2})]^2-\left[1+\frac{q^2}{m_0^2c^2}(A_0^2+A_1^2)\right]\right]\right\} \tag{20}$$

for $\sin(\psi_{s2})<0$ $(\pi<\psi_{s2}<2\pi)$.

In the absence of electrostatic field, $\mathcal{K}(\psi)$ is a constant, and one simply has $\psi_{s2}=2\pi-\psi_{s1}$, which means that, provided ψ_{s1} is a solution of Eq. (19), $2\pi-\psi_{s1}$ must satisfy Eq. (20) too. Thus the number of the resonant points in this situation is either zero or two. However, the presence of electrostatic field would break this symmetry since $\mathcal{K}(\psi)$ is now dependent of ψ. It is ready to verify that if both the Eqs. (19) and (20) are of solutions, one has $\psi_{s2}>2\pi-\psi_{s1}$ for $qE_p>0$, which implies that the orbit is shifted rightward by the additional electrostatic field. Physically, this feature could be understood as the result of the fact that the applied electrostatic field increases the acceleration gradient in the acceleration zone and decreases the deceleration gradient in the deceleration zone of the wave-particle interaction. The solid curve d in Fig. 2 is just such a shifted orbit in the limit $\psi_{s2}\sim2\pi$. Obviously, the incorporation of electrostatic field could also

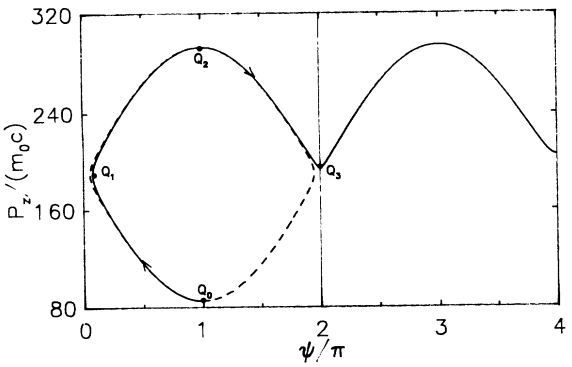

FIG. 3. Net acceleration mechanism for an electron moving in the $\mathcal{D}_4$ region shown in Fig. 2. The electron is injected at $\psi=\pi$ with initial $\beta_z=0.999\,932$. The parameters of the radiation field are the same as in Fig. 2. The dotted line shows the trajectory of the electron in the absence of static field. The solid line shows the same when $qE_p=1\times10^5$ eV/cm.

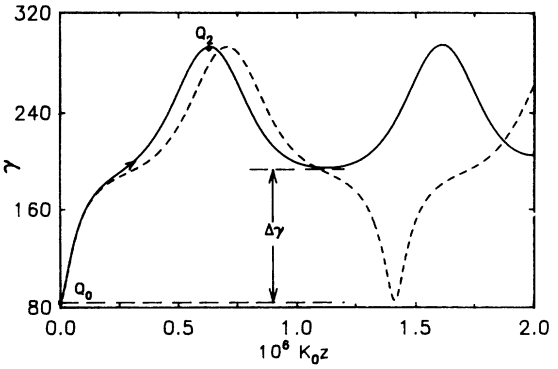

FIG. 4. Electron energy γ as a function of the traveling distance k_0z. The electron motion states referred to are the same as those in Fig. 3. The solid line shows the energy variation in the presence of electrostatic field, while the dotted line is for that in the absence of electrostatic field. $\Delta\gamma$ designates the low limit of the net acceleration.

lead to the emergence of electron trajectories with a single resonant point. It means that for a specific combination of field parameters and particle initial conditions, Eq. (19) has a solution, but there is no solution for Eq. (20). This situation corresponds to the trajectories in the region $\mathcal{D}_4$ in Fig. 2.

Now we examine more carefully the characteristics of the trajectories in different regions. For an electron moving in the $\mathcal{D}_1$ ($\mathcal{D}_3$) region, the condition

$$[\alpha(\psi)]^2-4\left[\frac{\omega_1}{\omega_0}\right]>0 \tag{21}$$

should hold for all ψ values in the interval $0-2\pi$. The electron longitudinal velocity continues to be faster (slower) than phase velocity β_ψ all along, and the electron phase continues to increase (decrease) when the electron travels in the field. In contrast to that, the trajectory for an electron in the region $\mathcal{D}_2$ is confined in a limited ψ space. Its longitudinal velocity oscillates around β_ψ, and the electron travels in a closed orbit in the P_z-ψ plane. In all three cases, no appreciable net acceleration can occur, if the interaction length is unlimited. Of great interest is the fact that the trajectory for an electron in the $\mathcal{D}_4$ region is totally asymmetrical with respect to $\psi=\pi$, and the electron can achieve net acceleration. Figure 3 presents a concrete example where the parameters of the radiation fields are the same as in Fig. 2. The dotted line denotes the trajectory of an electron injected at the point Q_0 with $\psi=\pi$ and $\beta_z=0.999\,932$ in the absence of an electrostatic field. The electron would travel along the closed orbit in the phase space, and could be of no net energy gain, unless the interaction were terminated abruptly. However, when a longitudinal electrostatic field with intensity $qE_p=1\times10^5$ eV/cm is incorporated, the electron turns to travel along the trajectory shown by the solid line. Since the initial velocity component $\beta_z<\beta_\psi$, the electron will first slip behind the potential and travel in the acceleration zone. After passing through the point Q_1, where $\beta_z=\beta_\psi$, and then Q_2, where $\psi\sim\pi$, the electron will arrive at point Q_3 where $\psi\sim2\pi$ but with $\beta_z>\beta_\psi$. Physically, this is due to the work done on the electron by the electrostatic field as it travels from Q_0 to Q_3. From then on, the electron, rather than returning to its original point Q_0, looks like a particle moving in the $\mathcal{D}_1$ region, and retains its β_z larger than β_ψ throughout the following process. The variation of the γ value of the electron is depicted as a function of k_0z by the solid line in Fig. 4, while the dotted line shows the variation without the electrostatic field. It can be seen from these figures that the electron would get a net energy $\Delta E\geq50$ MeV over the interaction length $k_0z\approx3.0\times10^4$. The averaged acceleration gradient is about $\Delta E/\Delta z\sim10^3$ MeV/m.

IV. SUMMARY

We have explored an alternative laser-based acceleration scheme where a moderate longitudinal electrostatic field is applied to achieve net acceleration in the IFEL's with electromagnetic wave wiggler. From the analytic solutions of the electron motion in the combined fields, we have found that the static field could lead to the appearance of a different kind of electron trajectory. The electrons following this kind of trajectory would extract net energy from the radiation fields. In the above given numerical example, the work done on the electrons by the electrostatic field is only 10 MeV/m, nearly two orders of magnitude less than that from the radiation fields. The role played by the static field in this scheme looks like a catalytic medium, which may transfer electrons to a new dynamic regime, making it available to get net acceleration. This interaction may also be viewed as a laser-assisted inverse bremsstrahlung acceleration. There are many questions left open to further discussion, such as the radiation loss, the transverse gradient, and diffraction effects of wave beam fields, the collective space charge effect, etc. We plan to study those questions in the future.

[1] Liang Feng and Yu-Kun Ho, Phys. Rev. E **47**, R2277 (1993).
[2] T. C. Katsouleas, in *High-Intensity-Laser Products,* edited by A. J. Alcock, SPIE Proc. Vol. 664 (SPIE, Bellingham, WA, 1986), p. 2, and references therein.
[3] R. B. Palmer, IEEE Trans. Nucl. Sci. **NS-28**, 3370 (1981)
[4] M. S. Hussein and M. P. Pato, Phys. Rev. A **46**, 3562 (1992).
[5] G.T. Moore, E. J. Bochove, and M. O. Scully, in *Nonlinear Optics and Materials,* edited by C. M. Bowden and C. D. Cantrell, SPIE Proc. Vol. 1497 (SPIE, Bellingham, WA, 1991), p. 323.
[6] T. C. Marshall, A. Bhattacharjee, S. Y. Cai, Y. P. Chou, and I. Wernick, Nucl. Instrum. Methods Phys. Res. Sect. A **304**, 683 (1991).
[7] I. Wernick and T. C. Marshall, Phys. Rev. A **46**, 3566 (1992).
[8] A. A. Chernikov and G. Schmidt, Phys. Rev. Lett. **68**, 1507 (1992).
[9] L. Cicchitelli, H. Hora, and R. Postle, Phys. Rev. A **41**, 3727 (1990).
[10] E. J. Bochove, G. T. Moore, and M. O. Scully, Phys. Rev. A **46**, 6640 (1992).
[11] M. O. Scully and M. S. Zubairy, Phys. Rev. A **44**, 2656 (1991).
[12] J. R. Fontana and R. H. Pantell, J. Appl. Phys. **54**, 4285 (1983).
[13] S. Varro and F. Ehlotzky, Phys. Rev. A **47**, 715 (1993).
[14] Anna K. Puntajer and C. Leubner, Opt. Commun. **73**, 153 (1989).